This is the peer reviewed author accepted manuscript (post print) version of a published work that appeared in final form in:

Ashiq, Ahmed, Sarkar, Binoy, Adassooriya, Nadeesh, Walpita, Janitha, Rajapaksha, Anushka Upamali, Ok, Yong Sik, Vithanage, Meththika 2019 'Sorption process of municipal solid waste biochar-montmorillonite composite for ciprofloxacin removal in aqueous media', Chemosphere, vol. 236, article no. 124384, pp. 1-11

This output may not exactly replicate the final published authoritative version for which the publisher owns copyright. It is not the copy of record. This output may be used for non-commercial purposes. This version is licensed under a Creative Commons CC-BY-NC-ND 4.0 license (http://creativecommons.org/licenses/by-nc-nd/4.0/).

The final definitive published version (version of record) is available at: https://doi.org/10.1016/j.chemosphere.2019.124384

Persistent link to the UniSA Research Outputs Repository: https://researchoutputs.unisa.edu.au/11541.2/28287

General Rights

Copyright and moral rights for the publications made accessible in the UniSA Research Outputs Repository are retained by the authors and/or other copyright owners and it is a condition of accessing publications that users recognize and abide by the legal requirements associated with these rights.

- Users may download and print one copy for the purpose of private study or research.
- You may not further distribute the material or use it for any profit-making activity or commercial gain
- You may freely distribute the persistent link identifying the publication in the UniSA Research Outputs Repository

If you believe that this document breaches copyright, please contact us and provide details. We will remove access to the work immediately and investigate your claim.

Sorption process of municipal solid waste biochar-montmorillonite composite for ciprofloxacin removal in aqueous media

Published in: *Chemosphere*

Citation for published version: Ashiq, A., Sarkar, B., Adassooriya, N., Walpita, J., Rajapaksha, A.U., Ok, Y.S., Vithanage, M., (2019) Sorption process of municipal solid waste biochar-montmorillonite composite for ciprofloxacin removal in aqueous media. *Chemosphere,* 236: 124384. doi: 10.1016/j.chemosphere.2019.124384.

Document version: Accepted peer-reviewed version.

Sorption process of municipal solid waste biochar-montmorillonite composite for ciprofloxacin removal in aqueous media

Ahmed Ashiq[1], Binoy Sarkar[2], Nadeesh Adassooriya[3], Janitha Walpita[1], Anushka Upamali Rajapaksha[1], Narayana Sirimuthu[4], Yong Sik Ok[5*], Meththika Vithanage[1, 6*]

[1]Ecosphere Resilience Research Centre, Faculty of Applied Science, University of Sri Jayewardenepura, Sri Lanka

[2]Department of Animal and Plant Sciences, The University of Sheffield, Sheffield, S10 2TN, United Kingdom

[3] Department of Food Science and Technology, Wayamba University of Sri Lanka, Makandura, Gonawila 60170, Sri Lanka

[4] Department of Chemistry, Faculty of Applied Science, University of Sri Jayewardenepura, Sri Lanka

[5] Korea Biochar Research Center, O-Jeong Eco-Resilience Institute (OJERI) & Division of Environmental Science and Ecological Engineering, Korea University, Seoul 02841, South Korea

[6]Molecular Microbiology and Human Diseases, National Institute of Fundamental Studies, Kandy 20000, Sri Lanka

*Co-corresponding authors:

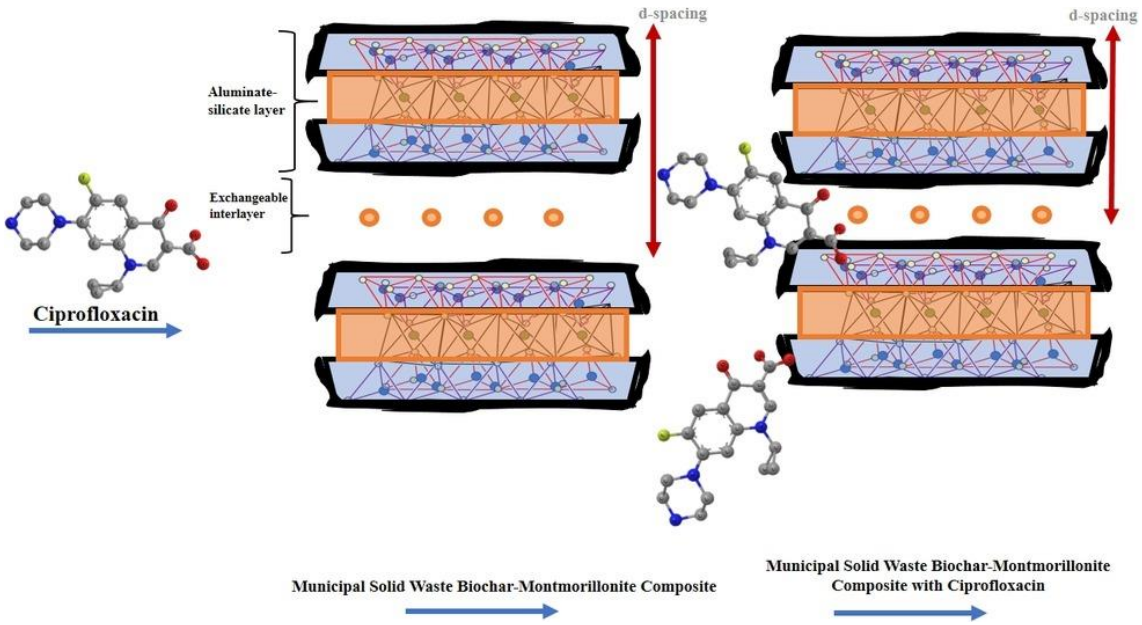
Prof. Yong Sik Ok; Korea University; E-mail: yongsikok@korea.ac.kr; and

Dr. Meththika Vithanage; University of Sri Jayewardenepura; E-mail: meththika@sjp.ac.lk

Highlights

- Biochar composite was prepared using municipal solid waste and montmorillonite.
- Ciprofloxacin adsorbed more efficiently on the composites than pristine materials.
- The primary mechanism for adsorption is π -induced electrostatic interactions.

Graphical abstract



Abstract

This study evaluates a novel adsorbent for ciprofloxacin (CPX) removal from water using a composite derived from municipal solid waste biochar (MSW-BC) and montmorillonite (MMT). The composite adsorbent and pristine materials were characterized using powder X-Ray Diffraction (PXRD), Fourier-Transform Infrared (FTIR) spectroscopy, and Scanning Electron Microscope (SEM) before and after the adsorption. Batch experiments were conducted to study the mechanisms involved in the adsorption process. Ciprofloxacin sorption mechanisms were interpreted in terms of its pH-dependency and the distribution coefficients. The SEM images confirmed the successful binding of MMT onto the MSW-BC through flaky structure along with a porous morphology. Encapsulation of MMT onto MSW-BC was exhibited through changes in the basal spacing of MMT via PXRD analysis. Results from FTIR spectra indicated the presence of functional groups for both pristine materials and the composite that were involved in the adsorption reaction. The Hill isotherm model and pseudo-second-order and Elovich kinetic models fitted the batch sorption data, which explained the surface heterogeneity of the composite and cooperative adsorption mechanisms. Changes made to the MSW-BC through the introduction of MMT, enhanced the active sites on the composite adsorbent, thereby improving its interaction with ionizable CPX molecules giving high sorption efficiency.

Keywords: Emerging contaminants, biochar, antibiotics, wastewater, pharmaceuticals

1. Introduction

The occurrence of antimicrobial agents in the environment is recognized as an emerging issue due to their recent identification and undesirable causative effects to the human health and

environment (Schmidt et al., 2012). Ciprofloxacin (CPX) is such an antibiotic: it is a fluorinated quinolone-based compound that has a broad spectrum antimicrobial activity (Ivanova et al., 2017). The antibiotics including CPX are non-detectable at times due to ultra-low concentrations, and are the least biodegradable, enabling them to persist in the environment for a long period of time. Ciprofloxacin has been found in treated wastewaters and groundwater at nanogram quantities that can cause bacterial resistance and disturb natural ecosystems (Kagle et al., 2009; Yan et al., 2013).

In aqueous media, like most ionizable antibiotics, CPX exhibits a pH-dependent behavior that allows it to coexist as differently charged species (Dai et al., 2012; Li et al., 2018). The pH dependency can directly influence the mitigation strategies to be used for the removal of antibiotics from the environment. This antibiotic has a carboxylic acid group on its third carbon and an amine group in the seventh carbon, and has pK_{a1} = 6.1 and pK_{a2} = 8.7, both of which significantly affect the existence of CPX species in water. As a result, the removal of CPX using appropriate adsorbents becomes challenging. When the pH is below 6.1, CPX exists as a cation due to the protonation of the amine group. When the pH is between 6.1 and 8.7, CPX exists in a zwitterionic state due to the simultaneous protonation and deprotonation of the amine and carboxylic acid groups, respectively. If the pH exceeds 8.7, the molecule exists as an anion due to deprotonation of the carboxylic group (Jiang et al., 2013; Li et al., 2014; Mondal et al., 2018). The protonation and deprotonation behaviors of CPX at different pH could affect the adsorption-desorption processes and enable different forms of the antibiotic to interact differently with the adsorbents. Therefore, adsorbing CPX by isolating it from aqueous media and binding it to the active sites of adsorbents becomes a challenging task. Plausibly, negatively charged adsorbents could bind closely with the protonated amine functional groups of CPX through coulombic attraction (Carmosini and Lee, 2009; Hu and Wang, 2016), and positively

charged adsorbents would bind with the deprotonated carboxylic or ketonic groups through complexation or hydrogen bonding reactions (Carmosini and Lee 2009; Li et al., 2018).

Obtaining a fundamental understanding of the sorption-desorption behavior of CPX in natural systems and its fate in the soil and water matrices has become a focus of research in the last decade and is essential for selecting an appropriate method of wastewater treatment. Several studies have focused on the adsorption of several other antibiotics that have a higher tendency of speciation under different aqueous conditions, especially under different pH of the system (Chang et al., 2016; Chang, Li, Yu, et al., 2009; Rajapaksha et al., 2014). Vasudevan et al. (Vasudevan et al., 2009) studied the pH-dependent sorption of CPX species in soils and suggested mechanisms accounting for high CPX sorption to different clay minerals. Such mechanisms included inner-sphere complexation, coulombic-attraction to the cationic amine groups of CPX, or cationic bridging with the carboxylic groups, creating a strong hydrogen bond (Ashiq et al., 2019; Hari et al., 2005; Vasudevan et al., 2009). Thus, clay minerals are widely used as adsorbents for CPX removal mainly due to their high cation exchange capacity, and their capabilities to remediate ionizable antibiotics, such as quinolones (Gu and Karthikeyan 2005a; Jiang et al., 2013; Wang et al., 2010).

However, using clay materials, especially montmorillonite (MMT) for CPX removal is challenging because of the gluey and exfoliating nature of the clay mineral which makes the separation of the adsorbent extremely difficult following the wastewater treatment. Furthermore, MMT in dried form is highly hydrophilic and attracts plenty of moisture turning the material into a sticky material which is not easy to handle (Madusanka et al., 2015; Premarathna et al., 2019; Yao et al., 2014). Carbon-based materials, such as biochar, have high surface-area, porosity and are produced from low-cost sources, including readily available biomaterials. As a potential adsorbent for organic contaminants with high retention rates, biochar is receiving global interests in environmental remediation applications (Ahmad et al.,

2014; Liu et al., 2015; Rajapaksha et al., 2014a). Thus, utilizing clay minerals and biochar together could be a viable option incorporating the properties of both the adsorbents into a single composite adsorbent and remediating a diverse range of contaminants.

Municipal waste has been a huge concern around the world, especially in the developing nations where the wastes are subjected to open dumping and deposited in landfills. It is estimated that the worldwide generation of solid wastes will see an increase from 1.3 billion tons per year up to 2.2 billion tons per year in 2025 (Hoornweg and Bhada-Tata, 2012). Biochar derived from municipal solid wastes has been studied so far sparsely, however they possess strong sorption characteristics for both organic and inorganic contaminants. The waste-derived biochar is known to have a surface which depends on the pH of the media and thus facilitate the removal of positive as well as negatively charged contaminant species (Gunarathne et al., 2019; Jayawardhana et al., 2019). The potential for removing compounds such as tetracycline and other ionizable antibiotics from water by biochar has even encouraged biochar amendments to soils for remediating the contaminants *in situ* (Jayawardhana et al., 2019; Peng et al., 2016; Vithanage et al., 2014). However, reports on the ability of biochar derived from municipal solid wastes to adsorb various species of antibiotics under different aqueous conditions are limited. The pore size of biochar can be often too small to accommodate large amphoteric molecules such as CPX (Peng et al., 2016).

Composites derived from municipal solid waste biochar (MSW-BC) and pure clay mineral, such as montmorillonite, are of topical interest when developing newly structured adsorbents to remove specialized ionizable adsorbates. The plausibility of exploring the properties of clay minerals for environmental remediation and incorporating them with carbon-based materials are yet to be examined in detail, especially for pharmaceutical contaminant remediation from aqueous media. The MMT is an aluminosilicate clay mineral, receiving interests for its widespread applications in material science. It is composed of two tetrahedral silica sheets

sandwiching one octahedral alumina sheet in between and contains exchangeable Na^+ and Ca^{2+} cations for structural charge neutrality in its lattice. The interlayer space between the sheets are occupied and held by those hydrated cations (e.g., Na^+, Ca^+), stabilizing the clay mineral structure and providing it with a high cation exchange capacity, high surface area, and swelling behavior that enables high adsorptivity (Carrado, 2004; Kenawy et al., 2016; Madusanka et al., 2017b). The MMT has been demonstrated to be a potential adsorbent for quinolone-based antibiotics through cation exchange, which is the prominent mechanism under environmental pH conditions (Jalil et al., 2017; Wu et al., 2010). However, pristine MMT as an adsorbent is very selective to the aqueous environment, and its surface alteration under highly heterogeneous aqueous environments might create unwanted features such as excessive exfoliation and glueyness. Hence, it has its own limitations for remediating antibiotic contamination, including the fact that it cannot be easily separated from the aqueous media (Aristilde et al., 2016). Therefore, composite materials that can adsorb a broad range of contaminants from heterogeneous aqueous environments are highly needed. Such composite materials could show high contaminant removal performance by combining the specific mechanisms of individual pristine materials, finally giving multifunctional adsorbents. The objective of this work is to investigate the plausibility and effectiveness of using a synthesized carbonaceous composite adsorbent for CPX removal from aqueous media and elucidate the possible mechanisms involved in CPX removal through modeling and adsorbent characterization studies. The CPX sorption properties of the composite derived from a sodium-exchanged MMT and a municipal solid waste biochar (MSW-BC) were tested under varying pH conditions. The plausible mechanisms of CPX sorption by the composite were also determined.

2. Experimental

2.1. Materials and chemicals

All reagents and chemicals were of analytical grade, from Sigma Aldrich, USA. All solutions were prepared using deionized water. Analytical-grade ciprofloxacin hydrochloride monohydrate was obtained from HIMEDIA Laboratories, India. Montmorillonite, Cloisite-Na^+ form, was obtained from Southern Clay, USA.

2.2. Biochar and biochar-montmorillonite composite preparation

The municipal solid waste was collected from Gohagoda Dumpsite, Kandy, Sri Lanka. Partially dried waste was collected, and the organic fractions were separated for biochar preparation. At a heating rate of 15 °C min^{-1}, the municipal solid waste was pyrolyzed up to 450 °C in a muffle furnace (Nabertherm, Germany) in a step-wise program, and then kept constant for about 4 h. The pyrolyzed municipal solid waste, now onward municipal solid waste biochar (MSW-BC), was immediately cooled by quenching with water at room temperature to activate the surface pores. The biochar was then oven-dried and sieved through a 2-mm mesh before using in further experiments. A mid-range temperature (450 °C) was maintained for the production of biochar for two reasons. Firstly, the lignin content in the municipal solid wastes was too low which makes the production yield small if pyrolyze at a high temperature (Bilgic et al., 2016; Demirbaş and Arin, 2002; Yang et al., 2017). Therefore, a mid-range temperature was selected to study the viability and applicability of maximized production yield while remediating CPX using the composite adsorbent (Premarathna et al., 2019b). Secondly, the ultimate goal of these experiments was to assess the potential of MSW-BC for the removal of various contaminants including potentially toxic metals and organic contaminants. Thus, a mid-value temperature range would prove practical for both trace metal and organic pollutant remediation.

Montmorillonite (50 g of MMT) was added to 2 L of deionized water to obtain a suspension, and the slurry was then shaken overnight (12 h) using a magnetic stirrer at a shaking speed of 150 rpm. The MSW-BC (50 g) prepared, was added and shaken further for 4 h under the same conditions. The clay-biochar slurry was then centrifuged, filtered, and oven dried at 60 °C for 12 h. The resulted composite (MSW-BC-MMT) was then sieved through a 2-mm sieve and used for experiments.

2.3. Characterization of biochar and biochar-montmorillonite composite

Powder X-ray diffraction (PXRD) measurements were conducted using a Rigaku, Ultima IV (Japan) diffractometer for both the pristine and composite materials to identify the crystalline phases in each sample. The X-ray diffractometer was operated at 40 kV and 40 mA, using the Cu Kα line at 1.54 A° as the radiation source. The specimen was powdered, dried, and placed on a glass slide for analysis. Each sample was scanned from 3° to 60° 2θ at a step size of 0.02 with a count time of 2.00 s at 25 °C. All high-intensity reflections for the pristine materials and composites were compared. Each of the patterns was characterized by the interlayer spacing (d-value) and the relative intensities of the predominant reflections. The interlayer spacing of each of the materials was calculated using the Bragg's law from the given 2 θ values.

The Fourier transform infrared (FTIR) spectra were acquired using a Thermo Scientific Nicolet iS10 spectrometer (USA) from 500 to 4000 cm^{-1} wavelength by accumulating 64 repetitive scans at a resolution of 4 cm^{-1} by using attenuated total reflection technique (ATR).

The specific surface area was determined using the Brunauer-Emmett-Teller (BET) method for the pristine MSW-BC and the MSW-BC-MMT composite using N_2 gas sorption analyzer (NOVA-1200, Quantachrome Corp., Boynton Beach, FL, USA).

Hitachi SU6600 analytical variable pressure Scanning Electron Microscope (Japan) was used to study the morphology of particles in the synthesized composite. The samples were mounted

213 on an aluminum pin stub with an additional thin layer of gold as a sputter coating, and images
214 were captured at different resolutions.

215 ## 2.4. Ciprofloxacin adsorption studies

216 A series of bottles were shaken with 1 g L^{-1} dosage of the two adsorbents – the pure MSW-BC
217 and the MSW-BC montmorillonite (MSW-BC-MMT) composite. As a general trend for most
218 adsorbents, the adsorption increases with an increase in the adsorbent dose. However, dosage
219 of 1 g L^{-1} was taken for the current study based on the literature data and targeting minimum
220 use of adsorbent for maximum removal of contaminant (Herath et al., 2016; Rajapaksha et al.,
221 2015, 2014b).

222 Stock solutions of known concentration of CPX (100 mg L^{-1}) were initially prepared, and a
223 certain known volume of the stock solution prepared was added to each batch to create a known
224 initial loading concentration. All the batch experiments were conducted at 25 °C under N_2-
225 purged environment sufficient to reduce the contamination of the working solutions by CO_2
226 present in the ambient air. After the experiment, the suspensions containing the CPX-loaded
227 adsorbents were centrifuged and filtered using syringe filters with a 0.45-µm cellulose acetate
228 membrane. The final CPX concentration of the clear filtrate was then analyzed using
229 UV/visible spectrophotometer (Shimadzu UV160A, Japan) at a wavelength of 280 nm (Wang
230 et al., 2010). All tests were conducted in triplicate.

231 ### *2.4.1. Edge experiment and distribution coefficient study*

232 For the pH sorption edge experiment, the initial concentration of CPX was kept as 25 mg L^{-1},
233 while the pH was varied from 4 to 9. The pH was adjusted with 0.1 M HNO_3 or 0.1 M NaOH
234 solutions. The adsorbents (pristine MMT, MSW-BC and MSW-BC-MMT) were maintained at
235 1 g L^{-1} dosage and overnight shaking (12 h) with a speed of 150 rpm. Once equilibrated, the
236 samples were centrifuged and filtered for the final CPX concentration analysis, as mentioned

above. The final concentration obtained at each pH value was used to calculate the distribution coefficient (K_d) values. The pristine MMT was studied to see the influence of pH on the K_d values concerning the MSW-BC-MMT composite.

To determine the mechanisms involved in the sorption of CPX onto different adsorbents used, the K_d values need to be computed at different pH levels. This facilitates the understanding of the contaminant behavior at the solid-solution interphase at a certain constant loading of CPX by observing the effect of different pH levels. The K_d value is calculated using the below equation Eq. (**Error! Reference source not found.**).

$$K_d = {q_{ads}}/{C_e} \quad (1)$$

where, q_{ads} (mg g^{-1}) is the adsorbed CPX on the adsorbents, and C_e (mg L^{-1}) is the concentration of CPX in the aqueous solution. The mechanism was then postulated for CPX adsorption by considering the pH effect.

2.4.2. Sorption kinetics

Sorption kinetic experiments were conducted for the removal of CPX at an adsorbent dosage of 1 g L^{-1} with a CPX concentration of 25 mg L^{-1} and a predetermined pH value (pH = 5 to 6) decided from the edge experiment. The contact times for the kinetic experiments were 5, 15, 30, 120, 240, 420, 600, 900, and 1440 min, and at the end of each run, the samples were analyzed for their final CPX concentrations, as described above.

2.4.3. Sorption isotherm

Sorption isotherm studies were carried out in different CPX concentration ranges (10 to 250 mg L^{-1}) at pH = 5-6, and solutions were equilibrated by overnight shaking (12 h). The other experimental conditions remain the same as those for the edges and kinetic experiments.

2.5. Data modeling and calculations

Non-linear kinetic models were used to describe the mechanisms involved in the adsorption of CPX by the pristine biochar and composite adsorbent. The pseudo-first order (Eq. 2), pseudo-second order (Eq. 3) and Elovich (Eq. 4) models were used:

Pseudo first order kinetics: $$q = q_e(1 - e^{-K_1 t}) \quad (2)$$

Pseudo-second order kinetics: $$q = \frac{K_2 q_e^2 t}{1 + K_2 q_e t} \quad (3)$$

Elovich kinetics: $$q = {}^{1}/_{b} \ln(ab) + {}^{1}/_{b} \ln(t) \quad (4)$$

where, q_e is the sorption capacity at equilibrium (mg g^{-1}), K_1 and K_2 are the rate constants of the pseudo-first and pseudo-second order models, respectively (g mg^{-1} min^{-1}), and t is the time in min (Ho and McKay, 1999). For the Elovich model, a is the initial sorption rate (g mg^{-1} min^{-1}), and b is the adsorption constant (g mg^{-1} min^{-1}) (Chien and Clayton, 1980).

The experimental isotherm data were fit using non-linear models, viz., Freundlich (Eq. 5), Langmuir (Eq. 6), Redlich-Peterson (Eq. 7), and Hills (Eq. 8) models to understand the physio-chemical mechanisms and validating the applicability of the adsorption process taking place between the solid-liquid interface.

Freundlich isotherm: $$q_e = K_f C_e^n \quad (5)$$

Langmuir isotherm: $$q_e = \frac{Q_m K_L C_e}{1 + K_1 C_e} \quad (6)$$

Redlich-Peterson Isotherm: $$q_e = \frac{k_R C_e}{1 + a C_e^b} \quad (7)$$

Hills Isotherm: $$q_{ads} = \frac{q_m (K_H C_e)^b}{1 + (K_H C_e)^b} \quad (8)$$

where C_e is the equilibrium concentration, q_{ads} is the amount of CPX adsorbed (mg g^{-1}), Q_m is the Langmuir maximum adsorption capacity (mg g^{-1}), K_L is the Langmuir equilibrium constant (L mol^{-1}), and n and K_F are Freundlich constants related to the non-linearity to the adsorption. For Redlich-Peterson's, k_R (L g^{-1}), a (L g^{-1}) and b (dimensionless) are constants. For Hill's, K_H is Hill constant and b is the empirical parameter variable with changing the heterogenous environment (Foo and Hameed, 2010). The parameter b should be greater than 1 for a positive interaction (Weerasooriya et al., 2006).

The Origin statistical package (version 8.0) was used for the analysis of data from batch adsorption experiments and material characterization methods.

3. Results and discussion

3.1. Characterization of MSW-BC and MSW-BC-MMT composite

3.1.1. PXRD analysis

The PXRD patterns of MSW-BC, CPX, MMT and MSW-BC-MMT composite (CPX treated and untreated) are shown in Fig. *1*. The oven dried MMT (60 °C) showed a d-value of 11.83 A° corresponding to the 001 basal reflection pattern of MMT at 2θ =7.43°. This is the characteristic reflection arising from the pristine MMT (Madusanka et al., 2017a). The MSW-BC pattern revealed the presence of quartz by showing a reflection at 2θ =23.76°, which was the only observable reflection of a crystallographic structural phase. When the MSW was heated over 450 °C, most mineral phases in MSW-BC exhibited amorphous characteristics and did not show an XRD reflection (Zhang et al., 2015; Zhang et al., 2015). The composite composed of the clay mineral and MSW-BC (i.e., MSW-BC-MMT) showed the characteristic reflections of the individual pristine materials, but with reduced intensity, and the

disappearance of the mineral phases indicated the structure to become more amorphous. The composite showed an increased interlayer spacing (d-value) of MMT (15.49 A°) as compared to the 11.83 A° value of the pristine MMT. This is likely due to the intercalation of organic molecules released from MSW-BC into the interlayer space of MMT, which can be further supported by the infrared spectroscopy results (Sinha Ray and Okamoto, 2003).

However, when CPX is introduced into the composite (i.e., MSW-BC-MMT-CPX), the spacing-value of the parent MMT was reduced to 14.46°. The surface active sites of the MMT most likely bound with the functional groups of CPX molecules as a result of a grafting reaction at the edges of the clay mineral plates, leading to the shrinkage of the interlayer space of MMT in the composite (Katti et al., 2008). This behavior was similar to that observed in a study where the antibiotic tetracycline adsorption on pure clay mineral was tested and the degree of interlayer swelling was analyzed with different initial tetracycline concentrations (Chang et al., 2009a).

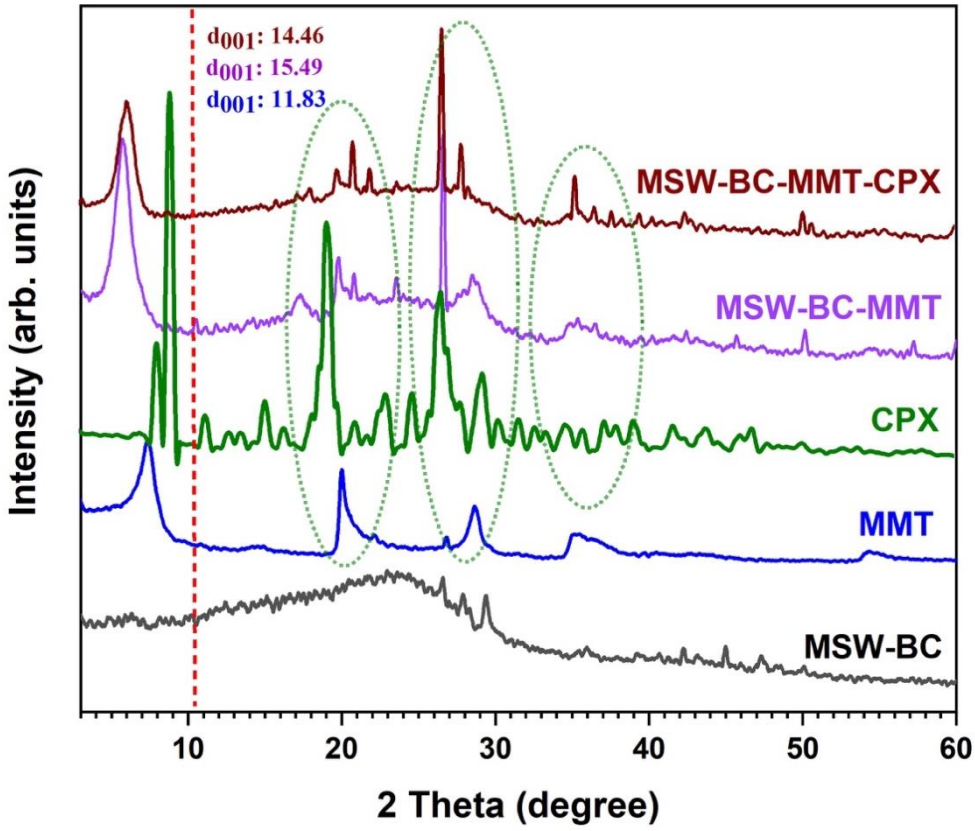


Fig. 1: PXRD patterns of MSW-BC, MMT, CPX pristine materials, and their composites

3.1.2. FTIR analysis

According to Fig. *2*, the transmission IR spectra exhibited characteristic bands in the region of 1200-1800 cm^{-1} for CPX (Jayawardhana et al., 2016). The C=O bands from the carboxylic group are located at approximately 1600-1700 cm^{-1}, and a significant peak is located at 1620 cm^{-1}, indicating the combined presence of C=C of the ring of CPX and C=C of MSW-BC. The hydration of the CPX and the other pristine materials during the solution/suspension preparation caused the presence of several other bands at 1500 cm^{-1}, indicating the existence of –OH groups (Madusanka et al., 2017a). Hydroxyl group stretching at 3650 cm^{-1} and Si-O stretching at 1050 cm^{-1} were the characteristics of MMT spectra. However, their broadening after the composites were prepared, suggests the intercalation of certain groups within the layers of the MMT causing a slight shift to the higher wavenumber region (Katti, Katti, and Dash 2008; Wu et al., 2018) (Fig. *2*). The disappearance of the C-H stretching band for the

pristine biochar observed at 2939 cm^{-1} in the spectra of the composite suggested that an aliphatic functional group was converted to aromatic functional group following the pyrolysis treatment, suggesting an arene ring formation in the biochar (Yan et al., 2014; Yu Wang et al., 2013). This was further supported through the postulated CPX adsorption mechanisms onto the MSW-BC-MMT composite at concerned pH values, which is unlikely to be seen in the case of CPX adsorption on the raw MSW-BC.

The C=C vibration band, which is characteristic of the pure CPX, at approximately 1620 cm^{-1} was not predominant in the CPX-loaded composites (Duan et al., 2018; Madusanka et al., 2015; Meng et al., 2009). There was no significant band of CPX in the spectra of the composites probably because the CPX concentration used in the experiments was not sufficient to visualize the changes in the spectra of the composites.

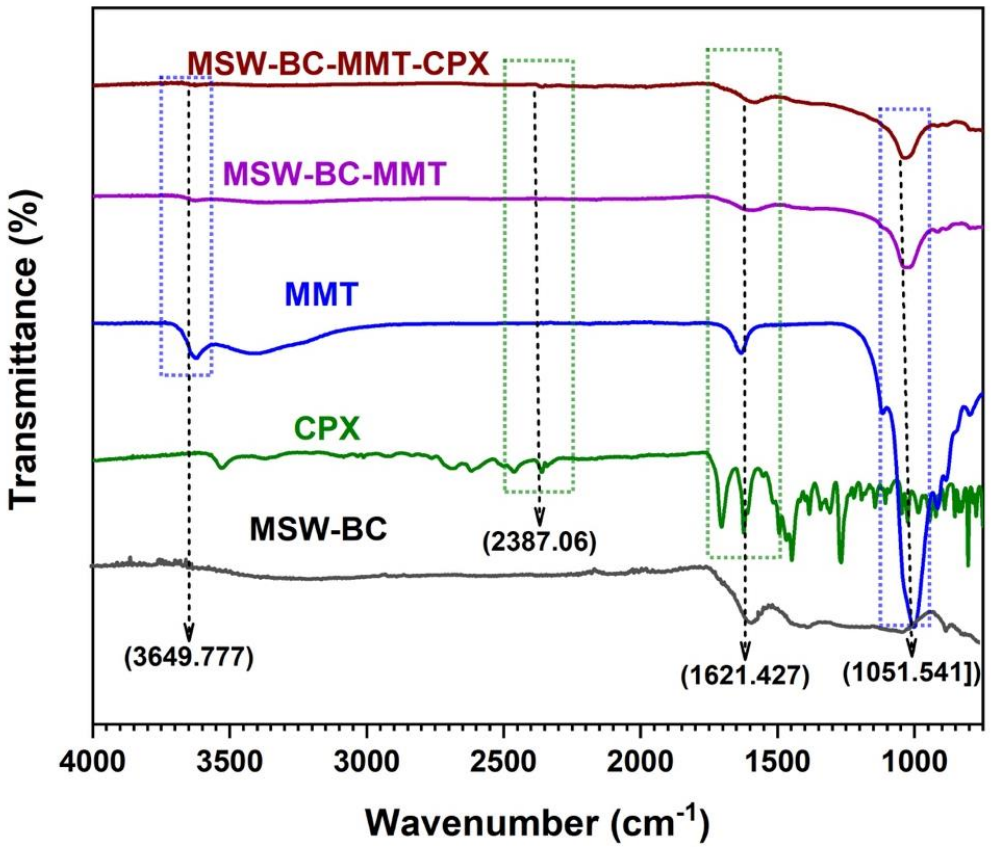


Fig. 2: FTIR spectra of pure MSW-BC, MMT and CPX along with their treated and untreated composites.

3.1.3. BET surface analysis

Table *1* shows the primary physicochemical characteristics of the adsorbents used for the study. The BET surface area of the composite increased when MMT was incorporated into the MSW-BC matrix. This was in accordance with the results obtained from the characterization studies (Fig. *1*-Fig. 3) and the distribution coefficient study (Fig. *4*). The specific surface area (SSA) of the pristine MMT and MSW-BC were 35.7 and 4.33 m^2 g^{-1}, respectively. The SSA of the MSW-BC-MMT composite was 6.51 m^2 g^{-1}, which was a drastic decrease in comparison to the pristine MMT likely due to the blockage of MMT pores following possible intrusion of carbonaceous nano-particles into the clay mineral lattices or pores during the slurry preparation (Chen et al., 2011). Although the SSA of the composite was smaller than MMT, the governing mechanisms for the adsorption of CPX were SSA-independent (Yang et al., 2019; Yu et al., 2016), as will be discussed in the remaining sections of this paper. In the current scenarios, most of the CPX adsorption was due to the functional sites present in the adsorbents, which are discussed further in the mechanism section and tallied with the obtained adsorption results below.

The pH of the MSW-BC-MMT composite was alkaline (pH=9.46), and slightly lesser than MSW-BC (pH=9.58) (Table *1*), likely due to the combined pH effect of the biochar and pristine MMT (pH=7.64). The basicity of biochar and biochar composite would have arisen from the presence of salts such as chlorides of potassium and calcium and oxygen-rich surface functional groups (as illustrated from the characterization results) (Peng et al., 2015; Usman et al., 2015). The raw biochar exhibited a high electrical conductivity (3450 µS cm^{-1}) due to the loss of volatile components via pyrolysis and the presence of different electrically conductive carbon lattices (Cantrell et al., 2012; Gai et al., 2014). Due to the high metallic elemental contents in the MMT, the electrical conductivity of the MSW-BC-MMT remarkably reduced as compared to the raw biochar (Table 1).

Table 1: Physicochemical characteristics of MSW-BC, MMT and MSW-BC-MMT composite

Adsorbents	Specific surface area (m^2 g^{-1})	pH	Electrical conductivity (μS cm^{-1})
MSW-BC	4.33	9.58	3450
MMT	35.75	7.64	1682
MSW-BC-MMT	6.51	9.46	1802

3.1.4. SEM analysis

Biochar derived from the municipal solid waste was a heterogeneous material consisting largely of organic materials, and therefore, was expected to have a random shape rather than an oriented structure in terms of its morphological features. SEM images of the pristine waste-derived MSW-BC and MSW-BC-MMT composite are shown in Fig. 3 at different magnifications. The presence of the MMT was confirmed from Fig. 3(c) and Fig. 3(d) and through the plate-like appearance at the cross-section, indicating the flaky structure that are unique for the clay mineral. The irregularities in the structure were due to the randomness of the pyrolyzed biochar as in Fig. 3(a) and Fig. 3(b), and the flaky appearance of the porous structure originated from MMT, confirming the binding of MMT plates with the carbonaceous material, i.e., biochar. The MMT embedded into the lattices of the biochar was visualized in the image (Fig. 3 (c) and Fig. 3(d)). However, due to the randomly evolved structure of the composite, the arrangement of the biochar and clay mineral particles was challenging to distinguish in the SEM images.

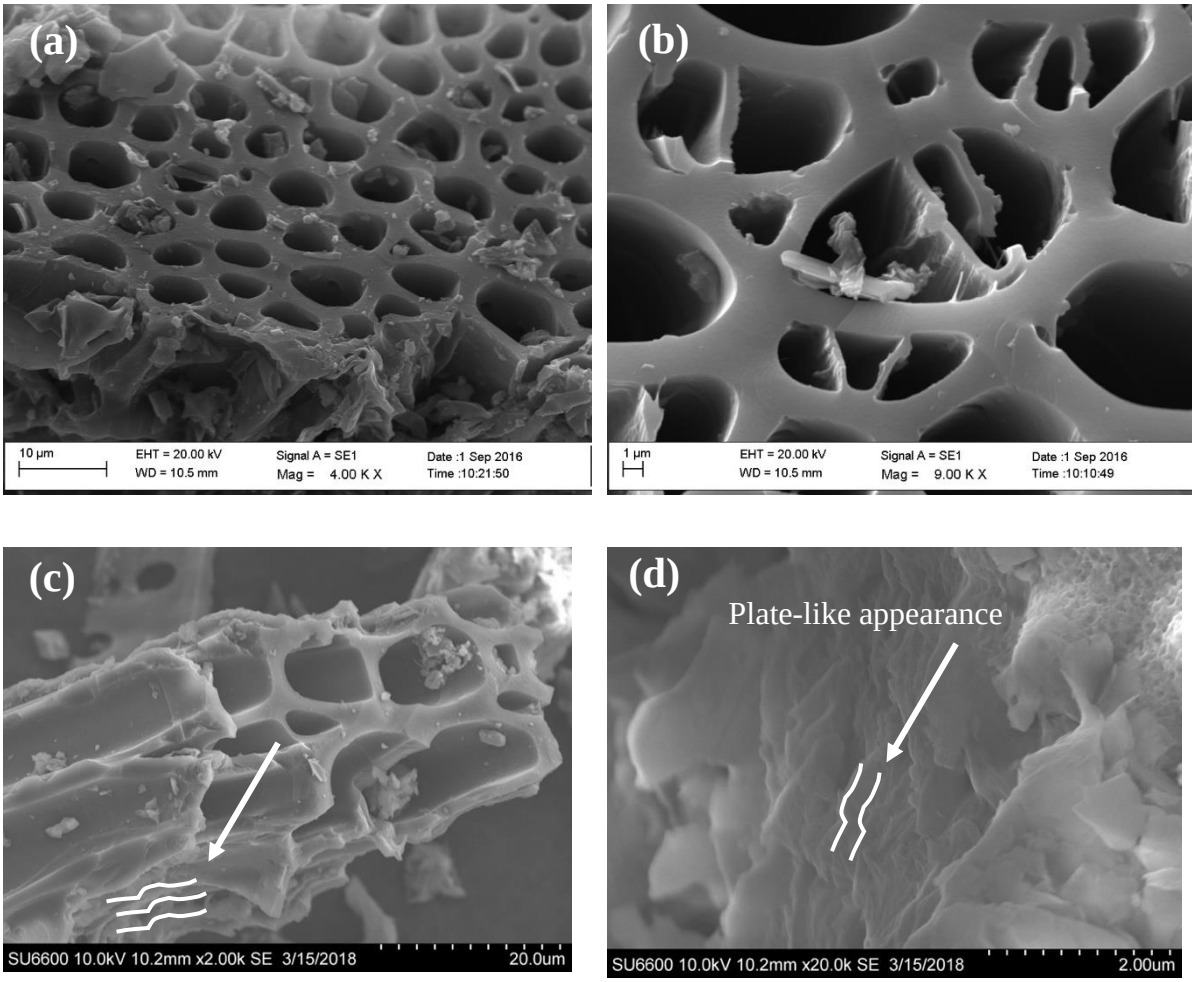


Fig. 3: SEM images of (a) MSW-BC magnification ×4.00k, (b) MSW-BC magnification ×9.00k, (c) MSW-BC-montmorillonite composite magnification ×2.00k and, (d) MSW-BC-montmorillonite composite magnification ×20.00k

3.2. Adsorption studies

3.2.1. Effect of initial solution pH

The calculated K_d values at different pH indicated a strong dependency of the adsorption process on pH which was due to the chemical speciation of the CPX molecules (cationic, anionic, and/or zwitterionic species) at different pH levels (Gu and Karthikeyan, 2005b).

The trends represented in Fig. *4* for both MSW-BC and MSW-BC-MMT were similar, at pH<5, K_d increased with increasing pH; however, at pH>5, K_d decreased as the pH increased. Due to different dissociation constants, the CPX molecules exist as cations when pH <6.1, and anionic at pH>8.7. The pK_a value from the carboxylic acid group of CPX is 6.1, and at pH<6.1, CPX

exists as a cation. CPX is zwitterionic at pH 6.1-8.7 (Gu and Karthikeyan, 2005a; Hari et al., 2005). This, in corroboration with the experimental results, explained the pH-dependent speciation of CPX with the surface charge characteristics of the adsorbents. The distribution for the composite was much lower than the pristine MMT that was attributed to the presence of MSW-BC.

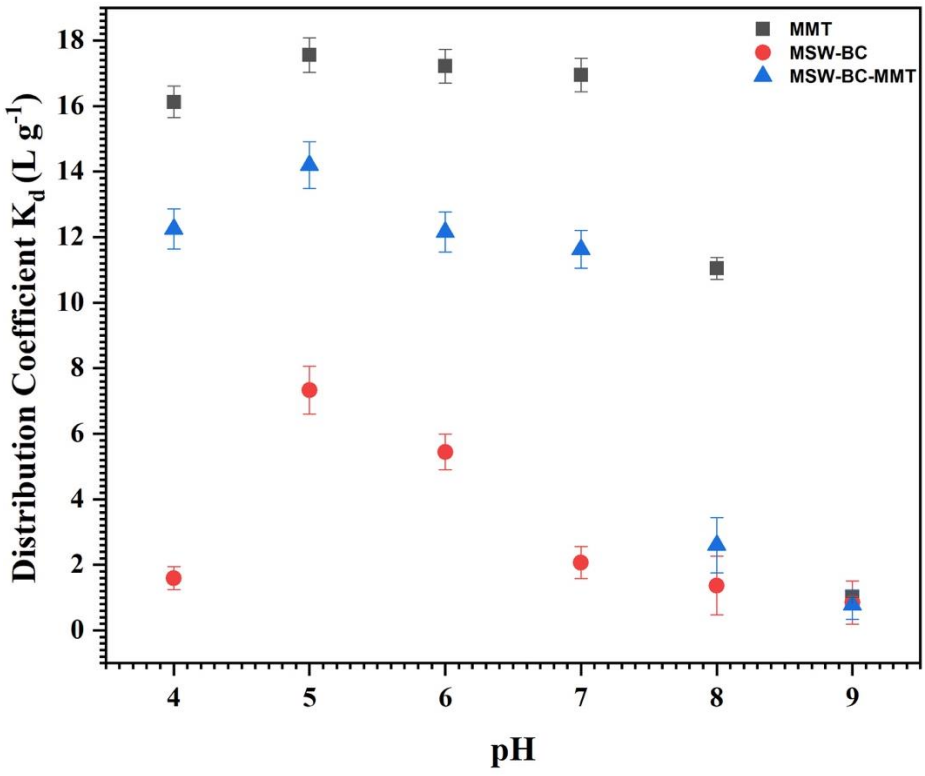


Fig. 4: Distribution coefficients (Kd) determined at pH values ranging from 4-9 for CPX adsorption on pure MMT, MSW-BC and MSW-BC-MMT composite

3.2.2. Effect of the initial concentration of CPX on adsorption

The increase in the CPX adsorption affinity with increasing concentration was clear in the isotherm plots (Fig. 5). The adsorption to MSW-BC did not reach equilibrium with increased concentration, however, for the MSW-BC-MMT composite showed increased affinity with increased CPX loading and then reached an equilibrium. The isotherm of CPX onto the pristine MSW-BC and MSW-BC-MMT composite showed best fits with the Hill isotherm (R^2~0.95). The Hill isotherm constants for CPX adsorption onto both pristine MSW-BC and MSW-BC-MMT composite were presented in table 2 along with their regression coefficients.

The maximum sorption was achieved when the initial CPX concentration was approximately 120 mg L^{-1}. The composite exhibited increased affinity with increased CPX loading and then reached at an equilibrium. The Hill equation postulates the binding of different species onto a homogeneous substrate. Adsorption is purely cooperative and is a phenomenon in which the solute or the ligand, when bonded at one site of the adsorbent directly, influences the consecutive active sites of the same adsorbent (Foo and Hameed, 2010; Ringot et al., 2007), and this attributes to an S-shaped sorption pattern. The forces of one CPX molecule, as the solute, with another CPX molecule at the adsorbent substrate's surface, is sufficient to lift the 'neighboring' molecule, and are cooperative (Giles et al., 1974). Hill coefficient 'b' provides the degree of cooperativity. If the coefficient exceeds 1, cooperativity is positive. The parameter 'b' should be greater than 1 for a positive interaction. Therefore, these data suggested that in this study, cooperative adsorption was the most probable mechanism of CPX removal. The MSW-BC-MMT composite had a higher maximum adsorption capacity (167.36 mg g^{-1}) by 1.5-fold than the adsorption of CPX on the pure MSW-BC. This is in relation to the results obtained from adsorbent characterizations that confirmed the possible CPX intercalation within the active sites of the composite.

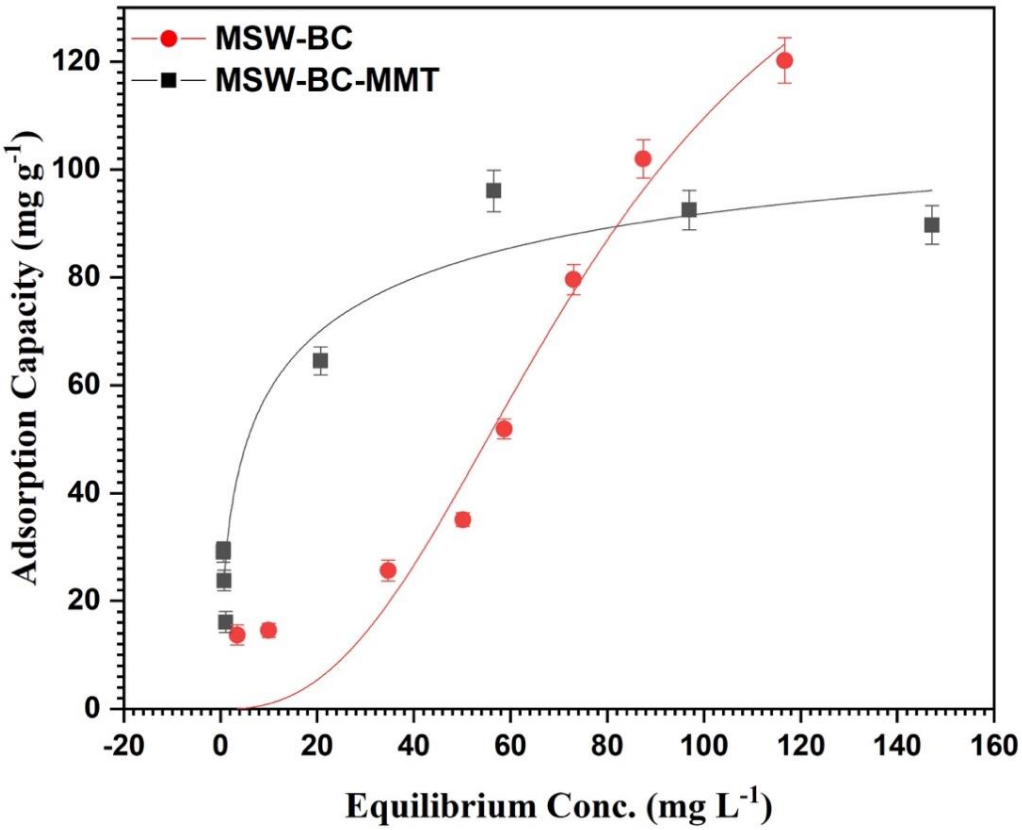


Fig. 5: Hill isotherm model fitting for the pure MSW-BC and MSW-BC-MMT composite at 1 g L^{-1} solid: solution ratio, 25°C, pH 5 and contact time of 12 h

Table 2: Hill isotherm parameters for CPX adsorption

Model	Parameter	Unit	MSW-BC	MSW-BC-MMT composite
Hills Isotherm	K_H	-	0.086	0.013
	q_m	mg g^{-1}	122.16	167.36
	b	L mg^{-1}	0.51	2.51
	r^2		0.94	0.95

3.2.3. Kinetic studies

The kinetic studies describe the CPX removal rate with the changes in the contact time of CPX on the solid-solvent interface (Naiya et al., 2009). The CPX transferring process from the solution to the adsorbents is simultaneously controlled by several processes, such as adsorption onto the surface, external diffusion, and/or pore diffusion, which can all be explained using adequate kinetic models (Kumar et al., 2008).

As shown in Fig. 6, the sorption rate of CPX on to both pristine biochar and biochar composite was initially fast, followed by a slower sorption until approaching the equilibrium plateau. Fast sorption during the first stage may be due to a large number of vacant sites available for sorption (Guo et al., 2013). The time taken to reach equilibrium for MSW-BC and MSW-BC-MMT were 200 and ~400 min, respectively. The adsorption by the MSW-BC-MMT composite was better than that by the pure MSW-BC, while the time taken to reach equilibrium was 2-fold greater than the pristine MSW-BC. Moreover, both adsorbents rapidly removed CPX in the beginning and then reached a plateau. These experimental data were analyzed using the pseudo-second order, pseudo-first order and Elovich models.

The kinetic data of pristine MSW-BC fitted well with the pseudo-second order model, with a regression coefficient of 0.98 (Table 3). The rate of the adsorption/desorption process controls the overall sorption mechanism when fitted in pseudo-second order model (Blanchard et al., 1984). In this model, the occurrence of surface adsorption through ion exchange between the substrate and the CPX molecules is widely agreed upon, with respect to the available sites for exchange (Plazinski et al., 2009). The adsorption of CPX by MSW-BC is purely chemisorption and is attributed to the different functional groups present in the active substrate.

The composite exhibited an Elovich fit, which described the effect of chemical reactions on the behavior of CPX adsorption with the surface substrate. The regression coefficient obtained for this fit was 0.95 (Table 3). The mechanism suggested by this fit is the formation of chemical bonds with the different functional group moieties of the CPX molecules (Jiang et al., 2013). The model assumes the heterogenous nature of the adsorbent surface with diverse functional groups and thus exhibits its own activation energy for the chemisorption to occur. Taking into account the surface functionalities of biochar (Lyubchik et al., 2016), Elovich model showed a higher degree of correlation for adsorption kinetics results. The available cationic sodium ions in the interlayers could easily bind with the amine groups of CPX, thereby isolating CPX from

the solution. Intercalation of CPX within the MMT could also be attributed to the ionic exchange mechanism, as postulated in this model (Wu et al., 2009).

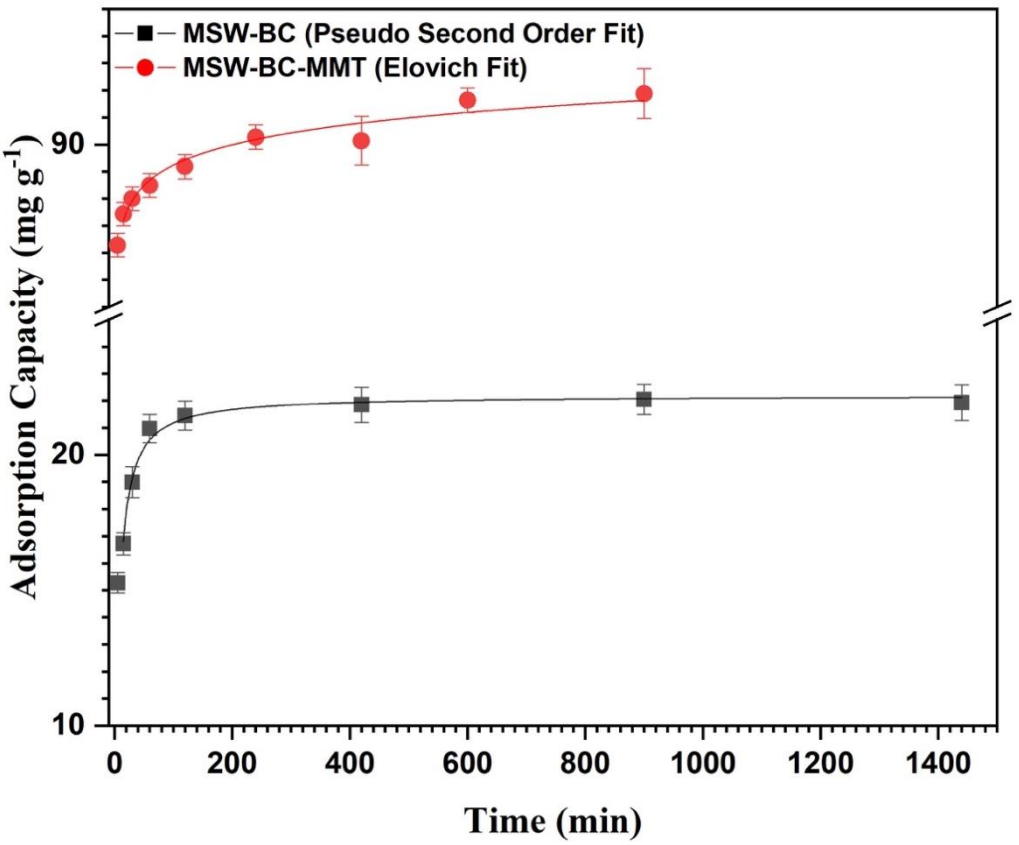


Fig. 6: Kinetic model parameters for CPX adsorption on MSW-BC and MSW-BC-MMT composite at 1 g L^{-1} solid: solution ratio, 25 °C, pH 5 and initial CPX concentration of 25 mg L^{-1}

Table 3: Kinetic model parameters for the adsorption of CPX onto pure MSW-BC and the MSW-BC-MMT composite

Model	**Adsorbents**		
	MSW-BC		
Pseudo-Second-Order	**Parameters**	**Unit**	
	K_2	g mg^{-1} min^{-1}	0.0093
	q_e	mg g^{-1}	22.19
	r^2		0.98
	MSW-BC-MMT		
Elovich	**Parameters**	**Unit**	
	a	g mg^{-1} min^{-1}	5.06×10^{33}
	b	g mg^{-1} min^{-1}	0.92
	r^2		0.95

3.3. Proposed adsorption mechanisms

The sorption of CPX was highly influenced by the system pH due to the existence of CPX in several forms, as described earlier (Zhang et al., 2010). Electrostatic interactions played a major role in CPX-adsorbent interfaces. According to the results obtained from the adsorption experiments, the composite showed enhanced removal of CPX. This was attributed to the cumulative effect coming from both MSW-BC and MMT (Yang et al., 2019; Yao et al., 2014).

Montmorillonite used as a natural adsorbent, is known for its high cation exchange capacity especially for inorganic and cationic contaminants. Biochar produced through carbonization of biomasses, on the other hand, is known for its multifunctional capabilities to remove a diverse pollutant types. Prominent mechanisms for the removal of CPX by the adsorbents used in this study included π-π electron donor interactions, electrophilic interactions, and hydrophobic interactions. From the edge experiment, the solution pH showed a strong influence on the adsorption capacity, and due to ionizable CPX molecules at different pH values, protonation and deprotonation reactions underwent simultaneously under acidic and alkaline conditions. This affected the CPX species present in the solution and their availability to adsorb.

From the results obtained, CPX could be adsorbed to the composite via π-π electron donor-acceptor interactions and π-cationic interactions that were attributed from the aromatic MSW-BC (Jayawardhana et al., 2016). The C=C vibration band observed at 1620 cm^{-1} and a shift towards the right after CPX sorption as noted in the FTIR spectrum along with the disappearance of 2939 cm^{-1} band in the composite were attributed to the π-π electron donor-acceptor interactions between the electron-rich biochar (arising from the arene groups) and electron-deficient CPX molecules (Jayawardhana et al., 2017; Peiris et al., 2017; Yan et al., 2014). Fig. 7 shows a brief scheme of π-π electron donor-acceptor interactions between the adsorbent and the aromatic CPX molecules, which could contribute to the adsorption of zwitterionic CPX. Available exchangeable cations in the MMT could plausibly interact with

the zwitterionic CPX molecules as well (Han et al., 2016; Li et al., 2018). Following are the predominant mechanisms postulated at the zwitterionic state of CPX:

$$\boldsymbol{CPX} - NH_2^+ + \boldsymbol{MSWBC} - A \leftrightharpoons \boldsymbol{CPX} - NH_2 - A - \boldsymbol{MSWBC}$$

$$\boldsymbol{CPX} - COO^- + \boldsymbol{MMT} - Na^+ \leftrightharpoons \boldsymbol{CPX} - COONa - \boldsymbol{MMT}$$

Where A is the arene unit that lies in the biochar (Peiris et al., 2017; Rajapaksha et al., 2014c), and the combination reaction are based on the functional groups present on the adsorbents. Thus, π- cationic bonds might form between the electron-rich adsorbent and the cationic CPX at lower pH, making it easier to isolate CPX from aqueous media and enhancing the adsorption capacity at a lower pH value. The oxygen-containing functional groups on CPX gets protonated at acidic environments through excessive H^+ ions, and the electrostatic attraction between the protonated cationic moiety of the CPX and the functional groups on the MSW-BC might control the sorption. Both effects cumulatively improved the adsorption ability.

The support from the SSA analysis is not up to the standpoint as the surface area is not the sole factor for adsorption, but a collective effect of the functional group's interactions between CPX and the adsorbents. From the PXRD analysis, it was noted that as CPX led to the shrinkage of the d-value of MMT, which could indicate the successful binding of CPX within the lattices of the MMT or free hydroxyls that caused a decrease of the interlayer spacing of the clay mineral. The strong interactions between the anionic moiety of CPX with the surface active sites of MMT layers led to the shrinkage of the interlayers as depicted in Fig. 7 (Madusanka et al., 2017a; Tran et al., 2015).

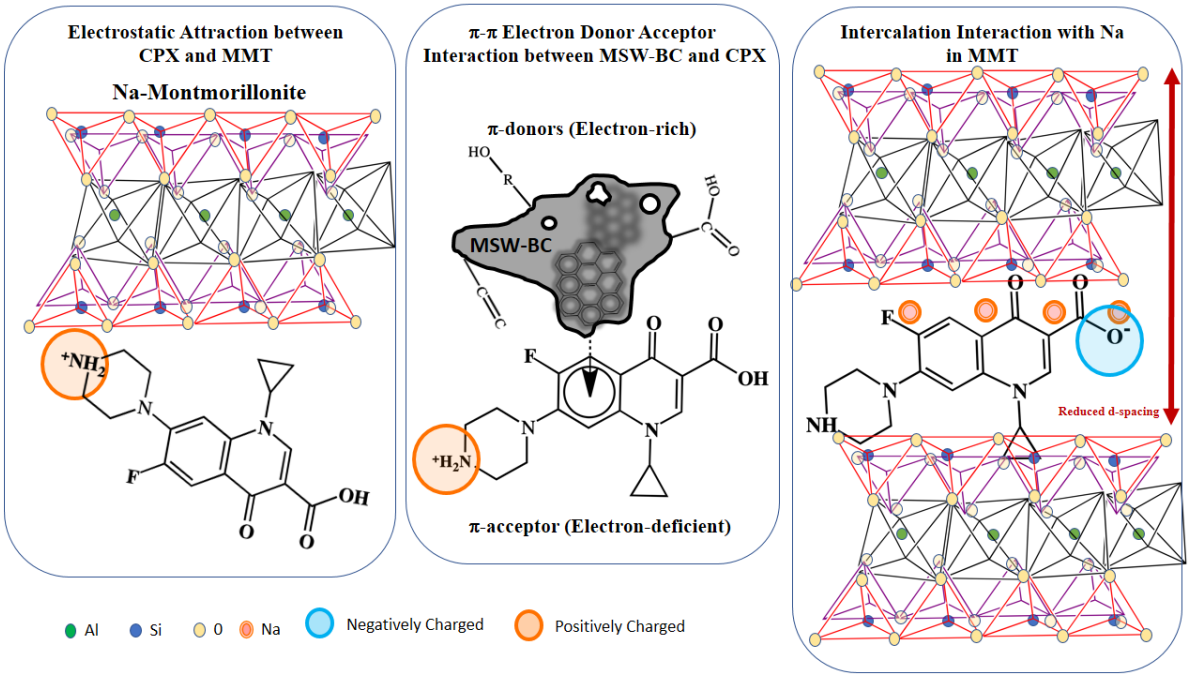


Fig. 7: Graphical scheme of possible ciprofloxacin adsorption mechanisms on to MSW-BC-MMT composite

However, at the zwitterionic state when both protonation of the amine functional groups and deprotonation of the carboxylic groups take place, the cationic exchange might appear as the major mechanism of CPX adsorption on MSW-BC-MMT composite. The active substrate of the MSW-BC-MMT composite, especially the exchangeable cations available at the MMT interlayers (Jiang et al., 2013), could bind strongly with the zwitterion/anionic CPX molecules, which further confirmed the mechanism as explained earlier where the available cationic sodium ions in the interlayers bound to the amine groups of CPX (Ahmed et al., 2017; Tareq et al., 2018).

4. Conclusions

The composite derived from municipal solid waste biochar and montmorillonite exhibited the highest CPX sorption as compared to the pristine adsorbents due to the enhanced active sites offered both from the biochar and the clay mineral. The removal of CPX was pH dependent. It could be concluded that the interaction of the composite with CPX was optimal under a range of environmental pH scenarios. Hill isotherm was fitted well suggesting a corporative

heterogeneous adsorption process onto the composite whereas chemical adsorption in heterogeneous surfaces was suggested by the kinetic data fitting into Elovich equation. The major governing mechanisms of CPX removal were facilitated by the FTIR and the PXRD characterization performed on the adsorbents. The proposed mechanism engaged in the adsorption of CPX with the composite comes from the combined cumulative effect from both the parent material: biochar and montmorillonite. The higher adsorption of the composites account for the adsorbent surface functional groups interactions and the adsorbate rather than the limited surface area. Thus, the composite was also environmentally sustainable as it re-utilized biomass solid wastes to make an adsorbent for environmental contaminants mitigation.

Acknowledgements

This work was supported by the Research Council grant [ASP/01/RE/SCI/2017/83] of University of Sri Jayewardenepura, Sri Lanka. Analytical support from the Instrument Centre, Faculty of Applied Sciences, University of Sri Jayewardenepura, Sri Lanka, is also acknowledged.

References

Ahmad, M., Rajapaksha, A.U., Lim, J.E., Zhang, M., Bolan, N., Mohan, D., Vithanage, M., Lee, S.S., Ok, Y.S., 2014. Biochar as a sorbent for contaminant management in soil and water: a review. Chemosphere.

Ahmed, M.B., Zhou, J.L., Ngo, H., Guo, W., Hasan Johir, A., Sornalingam, K., 2017. Single and competitive sorption properties and mechanism of functionalized biochar for removing sulfonamide antibiotics from water. Chem. Eng. J. 311, 348–358.

Aristilde, L., Lanson, B., Miéhé-Brendlé, J., Marichal, C., Charlet, L., 2016. Enhanced interlayer trapping of a tetracycline antibiotic within montmorillonite layers in the presence of Ca and Mg. J. Colloid Interface Sci. 464, 153–159.

Ashiq, A., Adassooriya, N.M., Sarkar, B., Rajapaksha, A.U., Ok, Y.S., Vithanage, M., 2019. Municipal solid waste biochar-bentonite composite for the removal of antibiotic ciprofloxacin from aqueous media. J. Environ. Manage. 236, 428–435.

Bilgic, E., Yaman, S., Haykiri-Acma, H., Kucukbayrak, S., 2016. Is torrefaction of polysaccharides-rich biomass equivalent to carbonization of lignin-rich biomass? Bioresour. Technol. 200, 201–207.

Blanchard, G., Maunaye, M., Martin, G., 1984. Removal of heavy metals from waters by means of natural zeolites. Water Res. 18, 1501–1507.

Cantrell, K.B., Hunt, P.G., Uchimiya, M., Novak, J.M., Ro, K.S., 2012. Impact of pyrolysis temperature and manure source on physicochemical characteristics of biochar. Bioresour. Technol. 107, 419–428.

Caporale, A.G., Pigna, M., Sommella, A., Conte, P., 2014. Effect of pruning-derived biochar on heavy metals removal and water dynamics. Biol. Fertil. Soils 50, 1211–1222.

562 Carmosini, N., Lee, L.S., 2009. Ciprofloxacin sorption by dissolved organic carbon from
563 reference and bio-waste materials. Chemosphere 77, 813–820.

564 Carrado, K.A., 2004. Handbook of layered materials. Basel.

565 Chang, P.-H., Jiang, W.-T., Li, Z., Kuo, C.-Y., Wu, Q., Jean, J.-S., Lv, G., 2016. Interaction
566 of ciprofloxacin and probe compounds with palygorskite PFl-1. J. Hazard. Mater. 303,
567 55–63.

568 Chang, P.H., Li, Z., Jiang, W.T., Jean, J.S., 2009a. Adsorption and intercalation of
569 tetracycline by swelling clay minerals. Appl. Clay Sci. 46, 27–36.

570 Chang, P.H., Li, Z., Yu, T.L., Munkhbayer, S., Kuo, T.H., Hung, Y.C., Jean, J.S., Lin, K.H.,
571 2009b. Sorptive removal of tetracycline from water by palygorskite. J. Hazard. Mater.
572 165, 148–155.

573 Chen, L.F., Liang, H.W., Lu, Y., Cui, C.H., Yu, S.H., 2011. Synthesis of an attapulgite
574 clay@carbon nanocomposite adsorbent by a hydrothermal carbonization process and
575 their application in the removal of toxic metal ions from water. Langmuir 27, 8998–
576 9004.

577 Chien, S.H., Clayton, W.R., 1980. Application of Elovich Equation to the Kinetics of
578 Phosphate Release and Sorption in Soils1. Soil Sci. Soc. Am. J. 44, 265.

579 Dai, C.M., Zhang, J., Zhang, Y.L., Zhou, X.F., Duan, Y.P., Liu, S.G., 2012. Selective
580 removal of acidic pharmaceuticals from contaminated lake water using multi-templates
581 molecularly imprinted polymer. Chem. Eng. J. 211–212, 302–309.

582 Demirbaş, A., Arin, G., 2002. An overview of biomass pyrolysis. Energy Sources 24, 471–
583 482.

584 Duan, W., Wang, N., Xiao, W., Zhao, Y., Zheng, Y., 2018. Ciprofloxacin adsorption onto

different micro-structured tourmaline, halloysite and biotite. J. Mol. Liq. #pagerange#.

Foo, K.Y., Hameed, B.H., 2010. Insights into the modeling of adsorption isotherm systems. Chem. Eng. J. 156, 2–10.

Gai, X., Wang, H., Liu, J., Zhai, L., Liu, S., Ren, T., Liu, H., 2014. Effects of Feedstock and Pyrolysis Temperature on Biochar Adsorption of Ammonium and Nitrate. PLoS One 9, e113888.

Giles, C.H., Smith, D., Huitson, A., 1974. A general treatment and classification of the solute adsorption isotherm. I. Theoretical. J. Colloid Interface Sci. 47, 755–765.

Gu, C., Karthikeyan, K.G., 2005a. Sorption of the antimicrobial ciprofloxacin to aluminum and iron hydrous oxides. Environ. Sci. Technol. 39, 9166–9173.

Gu, C., Karthikeyan, K.G., 2005b. Sorption of the antimicrobial ciprofloxacin to aluminum and iron hydrous oxides. Environ. Sci. Technol. 39, 9166–9173.

Gunarathne, V., Ashiq, A., Ramanayaka, S., Wijekoon, P., Vithanage, M., 2019. Biochar from municipal solid waste for resource recovery and pollution remediation. Environ. Chem. Lett.

Guo, X., Yang, C., Dang, Z., Zhang, Q., Li, Y., Meng, Q., 2013. Sorption thermodynamics and kinetics properties of tylosin and sulfamethazine on goethite. Chem. Eng. J. 223, 59–67.

Han, L., Ro, K.S., Sun, K., Sun, H., Wang, Z., Libra, J.A., Xing, B., 2016. New evidence for high sorption capacity of hydrochar for hydrophobic organic pollutants. Environ. Sci. Technol. 50, 13274–13282.

Hari, A.C., Paruchuri, R.A., Sabatini, D.A., Kibbey, T.C.G., 2005. Effects of pH and cationic and nonionic surfactants on the adsorption of pharmaceuticals to a natural aquifer

material. Environ. Sci. Technol. 39, 2592–2598.

Herath, I., Kumarathilaka, P., Al-Wabel, M.I., Abduljabbar, A., Ahmad, M., Usman, A.R.A., Vithanage, M., 2016. Mechanistic modeling of glyphosate interaction with rice husk derived engineered biochar. Microporous Mesoporous Mater. 225, 280–288.

Ho, Y.S., McKay, G., 1999. Pseudo-second order model for sorption processes. Process Biochem. 34, 451–465.

Hoornweg, Bhada-Tata, 2012. What a waste: a global review of solid waste management. [WWW Document]. URL https://siteresources.worldbank.org/INTURBANDEVELOPMENT/Resources/336387-1334852610766/What_a_Waste2012_Final.pdf

Hu, D., Wang, L., 2016. Adsorption of ciprofloxacin from aqueous solutions onto cationic and anionic flax noil cellulose. Desalin. Water Treat. 57, 28436–28449.

Ivanova, S., Dimitrova, D.J., Petrichev, M., 2017. Pharmacokinetics of ciprofloxacin in broiler chickens after single intravenous and intraingluvial administration. Maced. Vet. Rev. 40, 67–72.

Jalil, M.E.R., Baschini, M., Sapag, K., 2017. Removal of ciprofloxacin from aqueous solutions using pillared clays. Materials (Basel). 10, 1345.

Jayawardhana, Y., Gunatilake, S.R., Mahatantila, K., Ginige, M.P., Vithanage, M., 2019. Sorptive removal of toluene and m-xylene by municipal solid waste biochar: Simultaneous municipal solid waste management and remediation of volatile organic compounds. J. Environ. Manage. 238, 323–330.

Jayawardhana, Y., Kumarathilaka, P., Weerasundara, L., Mowjood, M., Herath, G., Kawamoto, K., Nagamori, M., Vithanage, M., 2016. Detection of benzene in landfill leachate from Gohagoda dumpsite and its removal using municipal solid waste derived

632 biochar. In: 6th International Conference on Structural Engineering and Construction
633 Management 2015, Kandy, Sri Lanka.

634 Jayawardhana, Y., Mayakaduwa, S.S., Kumarathilaka, P., Gamage, S., Vithanage, M., 2017.
635 Municipal solid waste-derived biochar for the removal of benzene from landfill leachate.
636 Environ. Geochem. Health 1–15.

637 Jiang, W.T., Chang, P.H., Wang, Y.S., Tsai, Y., Jean, J.S., Li, Z., Krukowski, K., 2013.
638 Removal of ciprofloxacin from water by birnessite. J. Hazard. Mater. 250–251, 362–
639 369.

640 Kagle, J., Porter, A.W., Murdoch, R.W., Rivera-Cancel, G., Hay, A.G., 2009. Biodegradation
641 of pharmaceutical and personal care products. Adv. Appl. Microbiol. 67, 65–108.

642 Katti, K.S., Katti, D.R., Dash, R., 2008. Synthesis and characterization of a novel
643 chitosan/montmorillonite/ hydroxyapatite nanocomposite for bone tissue engineering.
644 Biomed. Mater. 3.

645 Kenawy, E.R., Azaam, M., Saad-Allah, K., El-Abd, A., 2016. Preparation of organophilic
646 montmorillonite-based dimethylamino benzaldehyde-Schiff-base as antibacterial agents.
647 Arab. J. Chem.

648 Kumar, K.V., Porkodi, K., Rocha, F., 2008. Isotherms and thermodynamics by linear and
649 non-linear regression analysis for the sorption of methylene blue onto activated carbon:
650 Comparison of various error functions. J. Hazard. Mater. 151, 794–804.

651 Li, H., Zhang, D., Han, X., Xing, B., 2014. Adsorption of antibiotic ciprofloxacin on carbon
652 nanotubes: PH dependence and thermodynamics. Chemosphere 95, 150–155.

653 Li, J., Yu, G., Pan, L., Li, C., You, F., Xie, S., Wang, Y., Ma, J., Shang, X., 2018. Study of
654 ciprofloxacin removal by biochar obtained from used tea leaves. J. Environ. Sci. (China)
655 1–11.

656 Li, Y., Zeng, C., Wang, C., Zhang, L., 2018. Preparation of C@silica core/shell nanoparticles
657 from ZIF-8 for efficient ciprofloxacin adsorption. Chem. Eng. J. 343, 645–653.

658 Liu, W.J., Jiang, H., Yu, H.Q., 2015. Development of Biochar-Based Functional Materials:
659 Toward a Sustainable Platform Carbon Material. Chem. Rev. 115, 12251–12285.

660 Lyubchik, Svetlana, Lygina, E., Lyubchyk, A., Lyubchik, Sergiy, Loureiro, J.M., Fonseca,
661 I.M., Ribeiro, A.B., Pinto, M.M., Figueiredo, A.M.S., 2016. The Kinetic Parameters
662 Evaluation for the Adsorption Processes at "Liquid–Solid" Interface. In: Electrokinetics
663 Across Disciplines and Continents. Springer, pp. 81–109.

664 Madusanka, N., De Silva, K.M.N., Amaratunga, G., 2015. A curcumin activated
665 carboxymethyl cellulose-montmorillonite clay nanocomposite having enhanced
666 curcumin release in aqueous media. Carbohydr. Polym. 134, 695–699.

667 Madusanka, N., Sandaruwan, C., Kottegoda, N., Sirisena, D., Munaweera, I., De Alwis, A.,
668 Karunaratne, V., Amaratunga, G.A.J., 2017a. Urea–hydroxyapatite-montmorillonite
669 nanohybrid composites as slow release nitrogen compositions. Appl. Clay Sci. 150,
670 303–308.

671 Madusanka, N., Shivareddy, S.G., Eddleston, M.D., Hiralal, P., Oliver, R.A., Amaratunga,
672 G.A.J., 2017b. Dielectric behaviour of montmorillonite/cyanoethylated cellulose
673 nanocomposites. Carbohydr. Polym. 172, 315–321.

674 Meng, N., Zhou, N.L., Zhang, S.Q., Shen, J., 2009. Controlled release and antibacterial
675 activity chlorhexidine acetate (CA) intercalated in montmorillonite. Int. J. Pharm. 382,
676 45–49.

677 Mondal, S.K., Saha, A.K., Sinha, A., 2018. Removal of ciprofloxacin using modified
678 advanced oxidation processes: Kinetics, pathways and process optimization. J. Clean.
679 Prod. 171, 1203–1214.

680 Naiya, T.K., Bhattacharya, A.K., Das, S.K., 2009. Adsorption of Cd (II) and Pb (II) from
681 aqueous solutions on activated alumina. J. Colloid Interface Sci. 333, 14–26.

682 Peiris, C., Gunatilake, S.R., Mlsna, T.E., Mohan, D., Vithanage, M., 2017. Biochar based
683 removal of antibiotic sulfonamides and tetracyclines in aquatic environments: A critical
684 review. Bioresour. Technol. 246, 150–159.

685 Peng, B., Chen, L., Que, C., Yang, K., Deng, F., Deng, X., Shi, G., Xu, G., Wu, M., 2016.
686 Adsorption of Antibiotics on Graphene and Biochar in Aqueous Solutions Induced by π-
687 π Interactions. Sci. Rep. 6, 31920.

688 Peng, X., Hu, F., Lam, F.L.Y., Wang, Y., Liu, Z., Dai, H., 2015. Adsorption behavior and
689 mechanisms of ciprofloxacin from aqueous solution by ordered mesoporous carbon and
690 bamboo-based carbon. J. Colloid Interface Sci. 460, 349–360.

691 Plazinski, W., Rudzinski, W., Plazinska, A., 2009. Theoretical models of sorption kinetics
692 including a surface reaction mechanism: A review. Adv. Colloid Interface Sci. 152, 2–
693 13.

694 Premarathna, K.S.D., Rajapaksha, A.U., Adassoriya, N., Sarkar, B., Sirimuthu, N.M.S.,
695 Cooray, A., Ok, Y.S., Vithanage, M., 2019a. Clay-biochar composites for sorptive
696 removal of tetracycline antibiotic in aqueous media. J. Environ. Manage. 238, 315–322.

697 Premarathna, K.S.D., Rajapaksha, A.U., Sarkar, B., Kwon, E.E., Bhatnagar, A., Ok, Y.S.,
698 Vithanage, M., 2019b. Biochar-based engineered composites for sorptive
699 decontamination of water: A review. Chem. Eng. J. 372, 536–550.

700 Rajapaksha, A.U., Vithanage, M., Ahmad, M., Seo, D.C., Cho, J.S., Lee, S.E., Lee, S.S., Ok,
701 Y.S., 2015. Enhanced sulfamethazine removal by steam-activated invasive plant-derived
702 biochar. J. Hazard. Mater. 290, 43–50.

703 Rajapaksha, A.U., Vithanage, M., Lim, J.E., Ahmed, M.B.M., Zhang, M., Lee, S.S., Ok,

704 Y.S., 2014a. Invasive plant-derived biochar inhibits sulfamethazine uptake by lettuce in
705 soil. Chemosphere 111, 500–504.

706 Rajapaksha, A.U., Vithanage, M., Zhang, M., Ahmad, M., Mohan, D., Chang, S.X., Ok, Y.S.,
707 2014b. Pyrolysis condition affected sulfamethazine sorption by tea waste biochars.
708 Bioresour. Technol. 166, 303–308.

709 Rajapaksha, A.U., Vithanage, M., Zhang, M., Ahmad, M., Mohan, D., Chang, S.X., Ok, Y.S.,
710 2014c. Pyrolysis condition affected sulfamethazine sorption by tea waste biochars.
711 Bioresour. Technol. 166, 303–308.

712 Ringot, D., Lerzy, B., Chaplain, K., Bonhoure, J.P., Auclair, E., Larondelle, Y., 2007. In vitro
713 biosorption of ochratoxin A on the yeast industry by-products: Comparison of isotherm
714 models. Bioresour. Technol. 98, 1812–1821.

715 Schmidt, S., Winter, J., Gallert, C., 2012. Long-term effects of antibiotics on the elimination
716 of chemical oxygen demand, nitrification, and viable bacteria in laboratory-scale
717 wastewater treatment plants. Arch. Environ. Contam. Toxicol. 63, 354–364.

718 Sinha Ray, S., Okamoto, M., 2003. Polymer/layered silicate nanocomposites: A review from
719 preparation to processing. Prog. Polym. Sci. 28, 1539–1641.

720 Tareq, R., Akter, N., Azam, M.S., 2018. Biochars and Biochar Composites, Biochar from
721 Biomass and Waste. Elsevier Inc.

722 Tran, L., Wu, P., Zhu, Y., Liu, S., Zhu, N., 2015. Comparative study of Hg(II) adsorption by
723 thiol- and hydroxyl-containing bifunctional montmorillonite and vermiculite. Appl. Surf.
724 Sci. 356, 91–101.

725 Usman, A., Sallam, A., Zhang, M., Vithanage, M., Ahmad, M., Al-Farraj, A., Ok, Y.S.,
726 Abduljabbar, A., Al-Wabel, M., 2016. Sorption Process of Date Palm Biochar for
727 Aqueous Cd (II) Removal: Efficiency and Mechanisms. Water. Air. Soil Pollut. 227,

449.

Usman, A.R.A., Abduljabbar, A., Vithanage, M., Ok, Y.S., Ahmad, Mahtab, Ahmad, Munir, Elfaki, J., Abdulazeem, S.S., Al-Wabel, M.I., 2015. Biochar production from date palm waste: Charring temperature induced changes in composition and surface chemistry. J. Anal. Appl. Pyrolysis 115, 392–400.

Vasudevan, D., Bruland, G.L., Torrance, B.S., Upchurch, V.G., MacKay, A.A., 2009. pH-dependent ciprofloxacin sorption to soils: Interaction mechanisms and soil factors influencing sorption. Geoderma 151, 68–76.

Vithanage, M., Rajapaksha, A.U., Tang, X., Thiele-Bruhn, S., Kim, K.H., Lee, S.E., Ok, Y.S., 2014. Sorption and transport of sulfamethazine in agricultural soils amended with invasive-plant-derived biochar. J. Environ. Manage. 141, 95–103.

Wang, C.J., Li, Z., Jiang, W.T., Jean, J.S., Liu, C.C., 2010. Cation exchange interaction between antibiotic ciprofloxacin and montmorillonite. J. Hazard. Mater. 183, 309–314.

Wang, Y., Hu, Y., Zhao, X., Wang, S., Xing, G., 2013. Comparisons of Biochar Properties from Wood Material and Crop Residues at Different Temperatures and Residence Times. Energy & Fuels 27, 5890–5899.

Wang, Y., Yin, R., Liu, R., 2014. Characterization of biochar from fast pyrolysis and its effect on chemical properties of the tea garden soil. J. Anal. Appl. Pyrolysis 110, 375–381.

Weerasooriya, R., Seneviratne, W., Kathriarachchi, H.A., Tobschall, H.J., 2006. Thermodynamic assessment of Hg (II)–gibbsite interactions. J. Colloid Interface Sci. 301, 452–460.

Wijesekara, S.S.R.M.D.H.R., Mayakaduwa, S.S., Siriwardana, A.R., de Silva, N., Basnayake, B.F.A., Kawamoto, K., Vithanage, M., 2014. Fate and transport of pollutants through a

752 municipal solid waste landfill leachate in Sri Lanka. Environ. Earth Sci. 72, 1707–1719.

753 Wu, F.C., Tseng, R.L., Juang, R.S., 2009. Characteristics of Elovich equation used for the
754 analysis of adsorption kinetics in dye-chitosan systems. Chem. Eng. J. 150, 366–373.

755 Wu, Q., Li, Z., Hong, H., Yin, K., Tie, L., 2010. Adsorption and intercalation of
756 ciprofloxacin on montmorillonite. Appl. Clay Sci. 50, 204–211.

757 Yan, Y., Sun, S., Song, Y., Yan, X., Guan, W., Liu, X., Shi, W., 2013. Microwave-assisted in
758 situ synthesis of reduced graphene oxide-BiVO4 composite photocatalysts and their
759 enhanced photocatalytic performance for the degradation of ciprofloxacin. J. Hazard.
760 Mater. 250–251, 106–114.

761 Yang, X., Wan, Y., Zheng, Y., He, F., Yu, Z., Huang, J., Wang, H., Ok, Y.S., Jiang, Y., Gao,
762 B., 2019. Surface functional groups of carbon-based adsorbents and their roles in the
763 removal of heavy metals from aqueous solutions: A critical review.

764 Yang, X., Wang, H., Strong, P.J., Xu, S., Liu, S., Lu, K., Sheng, K., Guo, J., Che, L., He, L.,
765 Ok, Y.S., Yuan, G., Shen, Y., Chen, X., 2017. Thermal properties of biochars derived
766 from Waste biomass generated by agricultural and forestry sectors. Energies 10, 1–12.

767 Yao, Y., Gao, B., Fang, J., Zhang, M., Chen, H., Zhou, Y., Creamer, A.E., Sun, Y., Yang, L.,
768 2014. Characterization and environmental applications of clay–biochar composites.
769 Chem. Eng. J. 242, 136–143.

770 Yu, F., Li, Y., Han, S., Ma, J., 2016. Adsorptive removal of antibiotics from aqueous solution
771 using carbon materials. Chemosphere 153, 365–385.

772 Zhang, D., Pan, B., Zhang, H., Ning, P., Xing, B., 2010. Contribution of different
773 sulfamethoxazole species to their overall adsorption on functionalized carbon nanotubes.
774 Environ. Sci. Technol. 44, 3806–3811.

775 Zhang, J., Lü, F., Zhang, H., Shao, L., Chen, D., He, P., 2015. Multiscale visualization of the
776 structural and characteristic changes of sewage sludge biochar oriented towards
777 potential agronomic and environmental implication. Sci. Rep. 5, 9406.

778 Zhang, X., McGrouther, K., He, L., Huang, H., Lu, K., Wang, H., 2015. Biochar for organic
779 Contaminant Management in Soil. Biochar Prod. Charact. Appl. 140–165.

780